BEST AVAILABLE IMAGES

Defective images within this document are accurate representations of the original documents submitted by the applicant.

Defects in the images may include (but are not limited to):

- BLACK BORDERS
- TEXT CUT OFF AT TOP, BOTTOM OR SIDES
- FADED TEXT
- ILLEGIBLE TEXT
- SKEWED/SLANTED IMAGES
- COLORED PHOTOS
- BLACK OR VERY BLACK AND WHITE DARK PHOTOS
- GRAY SCALE DOCUMENTS

IMAGES ARE BEST AVAILABLE COPY.

As rescanning documents *will not* correct images, please do not report the images to the Image Problem Mailbox.

Journal of Membrane Science, 47 (1989) 91–106
Elsevier Science Publishers B.V., Amsterdam — Printed in The Netherlands

BUBBLE-FREE AERATION USING MEMBRANES: MASS TRANSFER ANALYSIS

PIERRE CÔTÉ*
Environment Canada, Wastewater Technology Centre, Burlington, Ontario L7R 4A6 (Canada)
JEAN-LUC BERSILLON and ALAIN HUYARD
Lyonnaise des eaux, Laboratoire central, Le Pecq (France)

(Received May 26, 1988; accepted in revised form March 24, 1989)

Summary

The mass transfer characteristics of silicone rubber hollow fibres for the oxygenation of water were studied. A resistance-in-series model with two resistances, the membrane and the liquid film resistances, was used to describe the oxygen transfer process. Data from the literature indicate that the liquid film resistance is normally larger than the membrane resistance when a polymer (such as silicone rubber) with a high oxygen permeability is used. A new module configuration, designed to decrease the liquid film resistance, was evaluated experimentally and compared with the conventional inside flow configuration. The module was very efficient in reducing the liquid film resistance. Experiments were also conducted to study the effect of oxygen partial pressure, the use of air or oxygen, the gas flow regime and the presence of surfactant on the efficiency of oxygen transfer.

Introduction

The development of thin gas-permeable membranes has stimulated research to evaluate their utilization for oxygen transfer to water. Bubble-free aeration can be achieved by placing a thin film of synthetic polymer between the gas and the liquid. Oxygen is transported through the membrane directly into solution.

Bubble-free aeration is desirable for some applications in wastewater treatment: (1) when the oxygen requirements are too high for conventional aeration systems, and (2) when bubbling of air would result in the stripping of volatile organic compounds or foaming of industrial wastewater. The purpose of this project was to investigate design and operation variables of bubble-free aeration at bench scale. While the scope of this paper is limited to mass transfer considerations, design equations and membrane aeration implementation case studies are presented in a companion paper by Côté et al. [1].

Bubble-free aeration is implemented using oxygen-permeable dense polymer or microporous membranes. With a dense polymer membrane, oxygen is

*Present address: Zenon Environmental Inc., 845 Harrington Ct., Burlington, Ontario L7N 3P3, Canada.

0376-7388/89/$03.50

absorbed in the polymer on the gas side and is transported by diffusion to the liquid. When a microporous membrane is used, the gas pressure is maintained below the bubble point; bubbles are formed at the surface of the membrane, but surface tension keeps them attached to it. Oxygen is transported through the pore system rather than through the polymer.

Schaffer et al. [2] were the first to report results of water aeration using polyethylene, ethylcellulose and polystyrene films. They noted that the already low oxygen transfer rates of the dry films were reduced by a factor of 5 to 10 when the films were immersed in water. The added resistance to transfer was attributed to the liquid film. Robb [3] studied the permeation properties of silicone rubber membranes and reported a very high permeability as compared with other polymers (Table 1). A comparison of the oxygen permeation properties of dense and porous membranes was carried out by Yasuda and Lamaze [4]. They found that wetting of the porous membrane significantly increased transfer resistance. With a porous membrane in which liquid water did not penetrate into the pores, the overall rate of transfer was comparable to that observed through the liquid boundary layer when using silicone rubber

TABLE 1

Oxygen permeability in various polymers (Ref. [3])

Polymer	Permeability[a] $(cm^3\text{-}cm/cm^2\text{-}sec\text{-}cmHg) \times 10^9$
Dimethyl silicone rubber	60
Fluorosilicone	11
Nitrile silicone	8.5
Natural rubber	2.4
Ethylcellulose	2.1
Polyethylene, low density	0.8
BPA polycarbonate	0.16
Butyl rubber	0.14
Polystyrene	0.12
Polyethylene, high density	0.10
Cellulose acetate	0.08
Methylcellulose	0.07
Poly(vinyl chloride)	0.014
Poly(vinyl alcohol)	0.010
Nylon 6	0.004
Poly(vinylidene fluoride)	0.003
Mylar	0.002
Kel F (unplasticized)	0.001
Vinylidene chloride-vinyl chloride	0.0005
Teflon	0.0004

[a]Multiply the numbers shown by 3.35×10^{-6} to obtain the units used in this paper, mol/m-sec-Pa.

membranes. Tang [5] studied oxygen transfer using silicone rubber tubes of various diameters and lengths. Water was circulated inside the tubes at various velocities while the outside of the tube was in contact with atmospheric air. The results demonstrated that, even with relatively thick membrane walls (241 to 371 μm), the mass transfer resistance of the liquid film represented more than 74% of the total resistance within the laminar regime. Experiments in the turbulent regime (Reynolds number up to 20,000) reduced the liquid film resistance to approximately 25% of the total resistance. A recent study in bubble-free aeration investigated the use of moving porous hydrophobic membranes [6]; the low bubble point of those membranes (13 mbar) however limited the gas pressure and, hence, the oxygen flux. Finally, Wilderer et al. [7] used reinforced silicone rubber tubes at a gas pressure of up to 7 bar to increase the oxygen transfer flux.

In this study, a novel approach was investigated to perform bubble-free aeration using dense polymer hollow fibre membranes. Gas was circulated inside the fibres and water was circulated transversely, on the shell side. This configuration allows oxygenation of liquids containing suspended solids and creates turbulence around the fibres at relatively low liquid velocity. The basic objectives of this study were, first, to develop a model to describe oxygen transfer through dense polymer membranes under various hydraulic conditions, and secondly to investigate the impact of the following experimental conditions on oxygen transfer: oxygen partial pressure, nature of the gas (oxygen/air), gas flow regime, surfactant and liquid velocity.

Background

The purpose of this section is to develop the relationships to express the oxygen flux using a resistance in series model and to enable the determination of mass transfer coefficients from measurements of dissolved oxygen concentrations.

Local overall mass transfer resistance

For dense polymer membranes, transport across the interface takes place via sorption/diffusion [8]. In addition to the membrane itself, there are resistances to mass transfer in the boundary layers that form in the gas and in the liquid, at the interface with the membrane. With reference to Fig. 1, the following expression for the oxygen flux is derived for steady-state conditions:

$$J=\frac{1}{\frac{1}{K_G}+\frac{1}{S_{MG}K_M}+\frac{1}{(S_{MG}/S_{ML})K_L}}\left(C_G-\frac{C_L}{S_{MG}/S_{ML}}\right) \quad (1)$$

where Cs are volumetric concentrations, Ks are mass transfer coefficients and

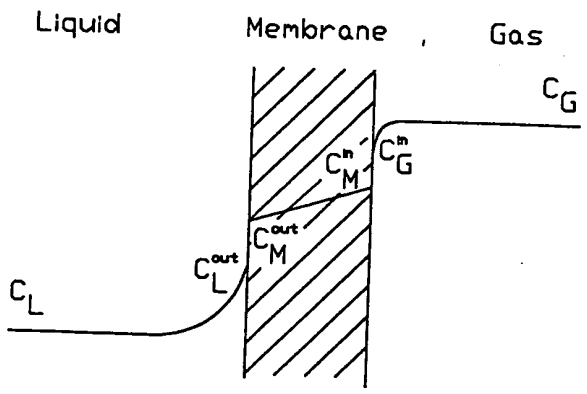

Fig. 1. Mass transfer model for membrane aeration.

Ss are dimensionless equilibrium partition coefficients representing the conditions at the interfaces:

$$S_{MG} = \frac{(C_M)_E}{(C_G)_E} \tag{2}$$

$$S_{ML} = \frac{(C_M)_E}{(C_L)_E} \tag{3}$$

Equation (1) represents a resistance-in-series model, which can be simplified by neglecting the gas film resistance: $1/K_G \ll 1/S_{MG}K_M \approx 1/(S_{MG}/S_{ML})K_L$. It can be expressed in more convenient units using Henry's law ($p=HC_L$) and the ideal gas law ($p=C_GRT$) to replace the gas concentrations in eqns. (1), (2) and (3) with partial pressure (p). As a result, eqn. (1) becomes

$$J = \frac{1}{\dfrac{1}{S'_{MG}K_M} + \dfrac{H}{K_L}} (p_G - HC_L) \tag{4}$$

where $S'_{MG} = S_{MG}/RT$ and has units of mol/m^3-Pa. The membrane mass transfer coefficient K_M can be expressed as [9]:

$$K_M = \frac{D_M}{\tau} \tag{5}$$

The product $S'_{MG}D_M$ is known as the permeability P for a gas–membrane–gas configuration:

$$P = S'_{MG}D_M \tag{6}$$

Finally, for hollow fibres, derivation of the flux equation in cylindrical coordinates leads to an expression where the membrane thickness is replaced by an equivalent thickness τ_e defined as [10]:

$$\tau_e = r_{out} \ln\left(\frac{r_{out}}{r_{in}}\right) \tag{7}$$

where r_{in} and r_{out} are, respectively, the inside and outside radius of the hollow fibre. When r_{out} is large as compared to $r_{out} - r_{in}$, $\tau_e \approx \tau$. Substituting eqns. (5), (6) and (7) into (4) and rearranging leads to:

$$J = \frac{1}{\frac{\tau_e}{PH} + \frac{1}{K_L}} \left(\frac{p}{H} - C_L\right) \tag{8}$$

The local overall mass transfer resistance $(1/K)$ is thus the sum of a membrane resistance (τ_e/PH) and a liquid film resistance $(1/K_L)$:

$$\frac{1}{K} = \frac{\tau_e}{PH} + \frac{1}{K_L} \tag{9}$$

Overall driving force

The driving force in eqn. (8), $p/H - C_L$, decreases over the length of a fibre, since the oxygen partial pressure (p) decreases as a result of headloss and oxygen transfer to the liquid. With reference to Fig. 2, the driving force can be expressed as a logarithmic average [11]:

$$(\Delta C)_{ln} = \frac{p_{in}/H - p_{out}/H}{\ln\left(\frac{p_{in}/H - C_L}{p_{out}/H - C_L}\right)} \tag{10}$$

It can be demonstrated that $(\Delta C)_{ln}$ can be substituted into eqn. (8) and used with the local overall mass transfer resistance of eqn. (9) to define an average flux over the length of the membrane [9]:

$$\bar{J} = K(\Delta C)_{ln} \tag{11}$$

Determination of the mass transfer coefficient

The local average transfer coefficient (K) can be determined from measurements of dissolved oxygen concentration as a function of time. A mass balance on a completely stirred tank reactor leads to:

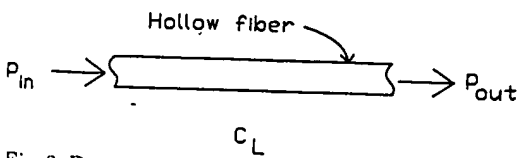

Fig. 2. Representation of the driving force for oxygen transfer from a hollow fibre to a completely stirred tank reactor.

$$\frac{dC_L}{dt} = Ka(p_G/H - C_L) \tag{12}$$

which can be integrated to obtain

$$\left[\frac{p_G/H - C_L(t)}{p_G/H - C_L(0)}\right] = e^{-Kat} \tag{13}$$

Equation (13) can be used to evaluate K from aeration experiments.

Experimental

Hollow fibre module

A membrane aeration module was constructed to ensure transverse liquid circulation on the shell side of the hollow fibres (Fig. 3). The module, 50 cm long by 10 cm external diameter, consisted of two Plexiglas headers joined by three stainless steel bars. In total, 43 hollow fibres were evenly distributed in an inner circle, 7.5 cm in diameter. The fibres had a total length of 44 cm and a length of 30 cm available for oxygen transfer. They were embedded in silicone mastic (Dow Corning RTV 612) and epoxy in each header to isolate the gas from the liquid.

The hollow fibres were dense silicone rubber Silastic fabricated by Dow Corning. Each fibre had an inside diameter of 305 μm and an outside diameter of 635 μm. The total external surface of transfer was therefore, 0.0258 m^2.

Experimental set-up

The experimental apparatus consisted of a covered tank (10 cm wide $\times$ 30 cm long $\times$ 50 cm high) in which the membrane module was placed between

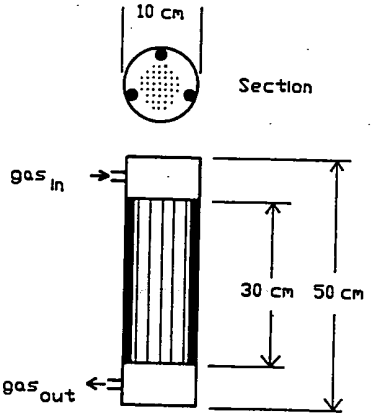

Fig. 3. Hollow fibre aeration model.

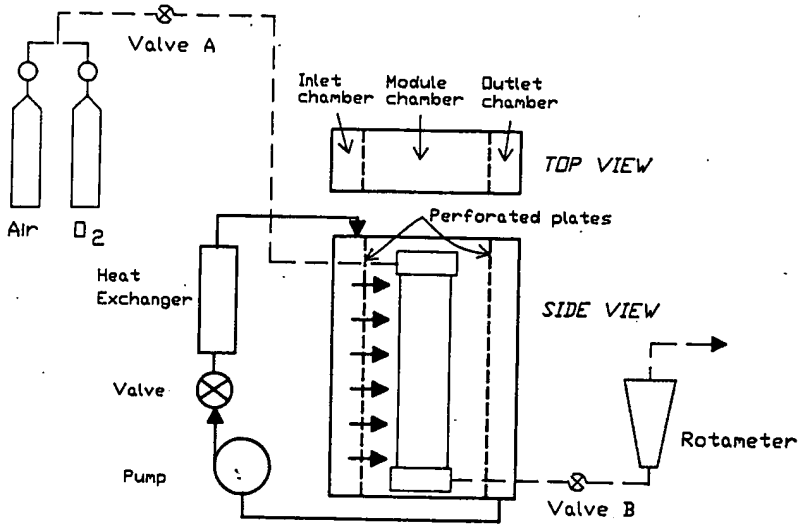

Fig. 4. Experimental set-up.

perforated plates to ensure horizontal flow perpendicular to the fibres (Fig. 4). Water was recirculated through an external pumping circuit consisting of a pump, a control valve, a heat exchanger and a flow meter. Two different pumping systems were used to obtain the tested range of water velocities in the module chamber: (1) small circuit, maximum velocity 2.28 cm/sec and total water volume 10.5 L, and (2) large circuit, maximum velocity 7.72 cm/sec and total water volume 16.0 L. The velocity was calculated based on the total flow rate and free cross-sectional area of flow past the fibres. The velocity profile across the module was verified by injecting a pulse of coloured tracer. In the module chamber, the plug flow was achieved; as a whole, the reactor could be considered a completely stirred tank reactor due to good mixing in the inlet and outlet chambers. The latter fact was desirable since it facilitated the analysis of the aeration experiments.

A dissolved oxygen probe and a thermometer were located in the outlet chamber and their output was monitored at discrete time intervals.

The gas distribution system consisted of a gas source (bottled oxygen or synthetic air), a pressure regulator, two high precision control valves, one on each side of the aeration module, pressure gauges and a rotameter (Fig. 4). The set-up allowed control of both the pressure and the gas flow rate through the aeration module. Some experiments were conducted in dead-end mode, with valve B closed (Fig. 4).

Experimental protocol

An experiment was conducted by carrying out the following steps:

1. The reactor was filled with tap water and the pump started. The flow rate of

cold water through the heat exchanger was adjusted to maintain a reactor water temperature of 20°C ± 1°C.
2. The water was deoxygenated by adding 60 mg/L of sulphite (as Na_2SO_3) and 0.2 mg/L of cobalt (as $CoCl_2 \cdot 6H_2O$).
3. For those runs requiring it, commercial soap containing 3.2% (by weight) of anionic surfactant (expressed as lauryl sulphate) was added.
4. The reactor was covered. The volume between the water surface and the cover (2–3 L) was purged with argon.
5. Aeration was started by adjusting the flow rate and pressure of air or oxygen. A flow rate of approximately 30 L/hr resulted in a linear velocity of 2.65 m/sec in the fibres (for an operating relative pressure of 1 bar).
6. When dissolved oxygen (DO) started to increase, readings of time and DO were taken frequently until the DO reached between 4 and 5 mg/L. The experimental set-up was designed and operated so that a run lasted between 10 min and 1 hr.

Results

Experimental conditions were selected to test a wide range of oxygen partial pressures using oxygen and air, to study the effect of the water and gas flow regimes on oxygen transfer and to observe the effect of surfactant addition. The experimental conditions and results of 37 runs are presented in Table 2. A liquid Reynolds number was calculated using the external fibre diameter as characteristic length ($Re = vd_{out}/\nu$). The local average mass transfer coefficients reported in Table 2 were calculated with eqn. (13) using the dissolved oxygen measurements $C_L(t)$ at the end of the experiment. This simple analysis was possible since the increase of C_L was linear over the duration of the experiment (due to a relatively large p_{in}/H value).

The mass transfer coefficients calculated from all experiments fall in a range from 11.3×10^{-6} to 34.4×10^{-6} m/sec. The observed variation was analyzed as a function of the following variables: oxygen partial pressure, nature of the gas, the gas flow regime, concentration of surfactant and liquid velocity. While the effects of the first four variables are best analyzed using the local average mass transfer coefficient K, the effect of liquid velocity will be examined using the liquid film mass transfer coefficient K_L calculated from eqn. (9).

Effect of oxygen partial pressure

The variation of the mass transfer coefficient as a function of oxygen partial pressure is shown in Fig. 5, using experiments conducted under the same hydraulic conditions. As expected, K is independent of oxygen partial pressure up to approximately 3 bar with an average $K = 28.3 \times 10^{-6}$ m/sec. However, for the two runs (140 and 142) conducted at higher pressure, the mass transfer coefficient dropped by approximately 18% to an average of 23.3×10^{-6} m/sec.

TABLE 2

Experimental conditions and results

Gas	Exp. no.	Pressure (bar)		Water velocity (cm/sec)	Liquid Reynolds number	K (m/sec$\times 10^6$)	Soap (mg/L)	Dead-end
		Total relative	Oxygen partial					
Oxygen	105	1.0	2.04	0.95	6.0	16.4	-	-
	106	1.0	2.04	0.48	3.1	14.7	-	-
	107	1.0	2.04	0.10	0.6	11.3	-	-
	108	1.0	2.04	0.48	3.1	15.4	-	-
	109	1.0	2.02	2.28	14.5	21.9	-	-
	110	1.0	2.02	1.49	9.5	20.4	-	-
	111	1.0	2.02	2.28	14.5	23.2	-	-
	112	1.0	2.02	2.28	14.5	22.4	-	-
	116	0.2	1.22	2.28	14.5	20.8	-	-
	120	1.0	2.01	7.72	49.0	27.8	-	-
	123	2.0	3.01	1.30	8.3	19.0	38.1	-
	124	2.0	3.01	1.30	8.3	20.3	38.1	-
	125	2.0	3.01	1.30	8.3	20.5	190.5	-
	126	2.0	3.01	1.30	8.3	21.3		-
	127	2.0	3.01	2.28	14.5	23.0	-	-
	128	2.0	3.01	2.28	14.5	24.5	190.5	-
	129	2.0	3.02	2.28	14.5	23.7	190.5	-
	130	2.0	3.02	2.28	14.5	23.8	190.5	-
	131	2.0	3.02	7.72	49.0	29.2	-	-
	132	2.0	3.02	7.72	49.0	31.4	190.5	-
	133	0.5	1.52	7.72	49.0	29.2	-	-
	134	0.5	1.52	7.72	49.0	34.4	190.5	-
	135	2.0	2.98	2.28	14.5	22.1	-	-
	136	2.0	2.98	2.28	14.5	11.7	-	yes
	137	2.0	2.98	2.28	14.5	12.4	-	yes
	138	2.0	2.98	7.71	49.0	14.9	-	yes
	139	2.0	2.98	7.71	49.0	17.2	-	yes
	140	3.0	4.02	7.71	49.0	22.8	-	-
	141	3.0	4.02	7.71	49.0	24.6	125.0	-
	142	4.0	5.02	7.71	49.0	23.7	-	-
	143	4.0	5.02	7.71	49.0	24.7	125.0	-
Air	113	2.0	0.64	2.28	14.5	16.6	-	-
	114	2.0	0.63	2.28	14.5	15.5	-	-
	118	2.0	0.64	2.28	14.5	20.6	-	-
	121	2.0	0.64	7.72	49.0	28.3	-	-
	122	2.0	0.64	7.72	49.0	27.2	-	-
	144	2.0	0.64	2.28	14.5	19.8	-	-

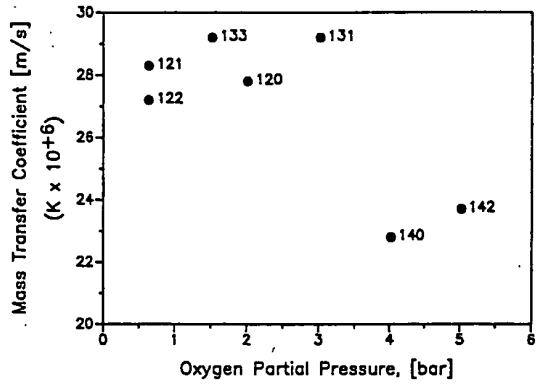

Fig. 5. Effect of gas pressure on the mass transfer coefficient.

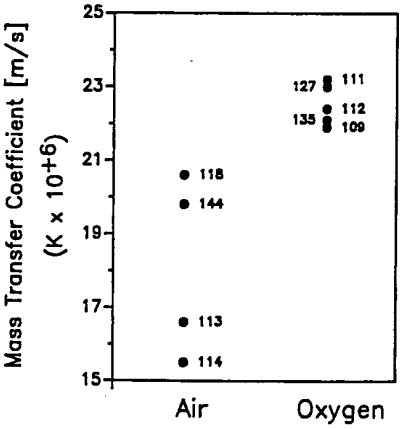

Fig. 6. Comparison of the mass transfer coefficient using air and oxygen.

The apparent decrease in performance at higher pressure is related to the observation of micro-bubbles on the surface of the fibres. These bubbles grew while attached to the surface of the fibres until they reached a critical size, then detached and escaped into the overlaying gas. The occurrence of this phenomenon is certainly related to the hydraulic conditions. At higher water velocity, oxygen would be more quickly removed from the surface of the fibres, preventing the partial pressure from exceeding the saturation point.

Effect of the nature of the gas

The effect of using air or oxygen on the mass transfer coefficient, under the same hydraulic conditions, is presented in Fig. 6. The five runs with oxygen are well grouped, with an average $K=22.5\times10^{-6}$ m/sec. The data are more

scattered for air; an average of $K = 18.1 \times 10^{-6}$ m/sec was observed, a decrease of 20% relative to oxygen.

The decrease in performance with air is attributed to the stripping of oxygen by bubbles of nitrogen that initially formed attached to the fibres and then escaped to the overlying gas. Since the water was initially saturated with nitrogen (at atmospheric pressure), the nitrogen permeating through the membrane readily came out of solution on the liquid side.

Effect of the gas flow regime

The performance of the fibre aerator operated in dead-end mode as compared to flow-through mode is presented in Fig. 7. The local average mass transfer coefficient dropped by 45% on average in dead-end mode.

This decrease in performance in dead-end mode is attributed to the fact that oxygen had to diffuse through the water vapour that filled the fibres. In flow-through mode, water vapour was readily evacuated from the fibres. This effect would be even more pronounced in a system with biological activity since, in addition to water vapour, carbon dioxide would be absorbed into the fibres. Furthermore, a decrease in temperature could cause condensation and a further decrease of performance.

Effect of surfactant

Adding commercial laundry soap to water increased the mass transfer coefficients (Fig. 8). Although the effect is relatively small (7% for $v = 2.28$ cm/sec and 20% for $v = 7.71$ cm/sec), it appears to be significant. The amount of soap added, 190.5 mg/L, is equivalent to approximately 6 mg/L of surfactant, expressed as lauryl sulphate, a concentration typical of that observed in wastewater [12].

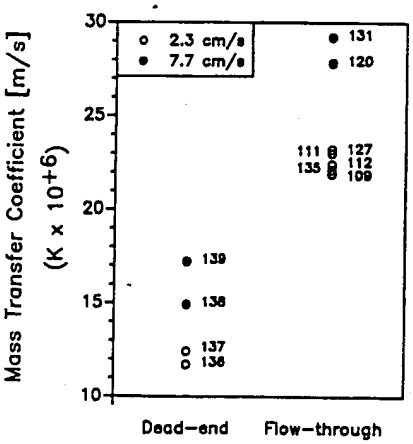

Fig. 7. Comparison of the mass transfer coefficient as a function of the gas hydraulic regime.

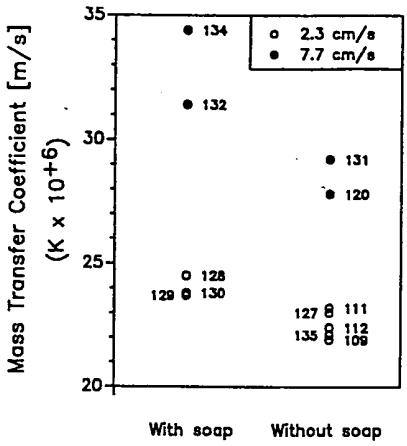

Fig. 8. The effect of surfactants on the mass transfer coefficients.

In bubble aeration, surfactants increase the liquid film resistance but produce smaller bubbles, increasing the transfer surface area and the detention time [13]. The overall effect depends on the aeration system (i.e., small or coarse bubbles).

In membrane aeration, only the first of the two effects mentioned above is applicable. Despite the expected increase in the liquid film resistance, it was observed in this work that addition of surfactant increased the overall transfer coefficient. This is attributed to the fact that silicone rubber is a highly hydrophobic material. Lowering the surface tension of water by the addition of soap thus allowed a better contact between the polymer and water.

Effect of liquid velocity

The effect of liquid velocity was studied using the data from the experimental runs performed with oxygen at a total pressure not exceeding 2 bar (relative), with gas flow through the fibres and without the addition of soap. Table 3 summarizes the experimental data meeting these conditions, together with results of calculations to obtain the liquid film resistance.

The Reynolds numbers and total resistances ($1/K$) were extracted from Table 2. The membrane resistance ($1/K_M = \tau_e/PH$) was calculated using the following values: $\tau_e = 234 \times 10^{-6}$ m [eqn. (7)], $P = 1.63 \times 10^{-13}$ mol/m-sec-Pa (permeability of oxygen provided by the manufacturer, differs slightly from that reported in Table 1) and H = 73,800 Pa-m^3/mol. The liquid film resistance was obtained by difference. The liquid film resistance is very sensitive to the hydraulic conditions, decreasing by a factor of 4.4 when the Reynolds number increases from 0.6 to 49, the range tested in this work. Column 6 of Table 3 represents the importance of the liquid film resistance as compared with the total resistance. It varies from 78.5% for $Re = 0.6$ to an average of 45.5% for

TABLE 3

Comparison of liquid film and membrane resistances

Exp. no.	Liquid Reynolds number	Resistance (sec/m)			Liquid/total (K/K_L, %)	Sherwood number
		Total ($1/K$)	Membrane ($1/K_M$)	Liquid ($1/K_L$)		
107	0.6	88,496	18,986	69,510	78.5	4.7
106	3.1	68,027	18,986	49,041	72.1	6.7
108	3.1	64,935	18,986	45,949	70.8	7.1
105	6.0	60,976	18,986	41,990	68.9	7.8
123	8.3	52,623	18,986	33,646	63.9	9.8
110	9.5	49,020	18,986	30,034	61.3	10.9
111	14.5	43,103	18,986	24,117	56.0	13.6
112	14.5	44,643	18,986	25,657	57.5	12.8
116	14.5	48,077	18,986	29,091	60.5	11.3
109	14.5	45,662	18,986	26,676	58.4	12.3
135	14.5	45,249	18,986	26,263	58.0	12.5
127	14.5	43,478	18,986	24,492	56.3	13.4
119	49.0	39,526	18,986	20,540	52.0	15.9
131	49.0	34,247	18,986	15,261	44.6	21.5
133	49.0	34,247	18,986	15,261	44.6	21.6
120	49.0	35,971	18,986	16,985	47.2	19.3

$Re = 49$. Finally, column 7 contains Sherwood numbers ($Sh = K_L d_{out}/D_L$) based on the liquid film mass transfer coefficients. Linear regression was used to derive the mass transfer correlation, $Sh = 0.61 Re^{0.363} Sc^{0.333}$ (imposing the 0.333 exponent to the Schmidt number). This correlation is similar to those reported by Yang and Cussler [14] from original work and from the heat transfer literature.

Maximizing fluxes in membrane aeration

Equation (4) indicates that two methods can be used to increase oxygen fluxes in membrane aeration: (1) decrease the mass transfer resistance, and (2) increase the driving force.

The mass transfer resistance is composed of two apparently independent terms, the membrane resistance and the liquid film resistance. The membrane resistance, in turn, depends on the polymer permeability to oxygen and on the membrane thickness. With a highly permeable polymer such as silicone rubber and membranes which could be thinner than those used in this work (165 μm), the membrane resistance would be much smaller than the liquid film resistance. Further efforts to reduce the mass transfer resistance should therefore be concentrated on improving the hydraulics of the membrane module.

Equation (4) indicates that the flux increases linearly with an increase of the driving force (i.e., the oxygen partial pressure on the gas side). However,

this work demonstrated that a linear relationship only holds up to a certain pressure which is a function of the efficiency of transfer on the liquid side. As the gas pressure increases, the concentration of oxygen in the liquid boundary layer also increases, up to a point where saturation is reached and bubbles form at the surface of the membrane. An increase in the gas pressure should therefore be matched with improvement of the hydraulics on the liquid side.

Conclusions

A new configuration for a membrane aerator was evaluated using silicone rubber hollow fibres with the liquid flowing transversely on the shell side.

Data from the literature and from this work were used to validate a two resistance in series model to describe oxygen transfer. According to this model, the liquid film resistance represented between 44.5 and 78.5% of the total resistance to transfer for the conditions tested in this work.

The shell/transversal flow configuration was very efficient in reducing the liquid film resistance, by a factor of 4.4 when the Reynolds number increased from 0.6 to 49.

The mass transfer coefficient was independent of oxygen partial pressure up to a partial pressure of 3 bar. At higher pressures, smaller coefficients were observed as oxygen concentration exceeded saturation at the membrane–liquid interface and formed micro-bubbles that came out of solution at the surface.

The use of air reduced the mass transfer coefficient by 20% when compared to oxygen because nitrogen degassing resulted in stripping of oxygen from the solution.

Operation of the aerator in dead-end mode resulted in a decrease in transfer rates of 45% as compared to the rates observed in flow-through mode.

Small increases in transfer rates were observed using water containing a concentration of surfactant typical of that in wastewater as compared to tap water. This was attributed to a better contact between water and the membrane.

Improvement of the oxygen fluxes could be obtained by decreasing the mass transfer resistance and using larger oxygen partial pressure. In doing so, care must be taken to keep the liquid film resistance and the membrane resistance approximately equal and to ensure that any increase in the oxygen partial pressure on the gas side is matched by a decrease in the liquid film resistance to avoid exceeding saturation and degassing at the membrane wall.

Acknowledgements

This work was conducted at the Central Laboratory of Lyonnaise des eaux, Le Pecq, France under a Eureka project entitled "Conception et fabrication de

membranes pour application au traitement des eaux" and was partially financed by the French Ministère pour la recherche supérieure, contrat 86.W.0426.

The first author was on leave from Environment Canada with a post-doctoral grant from the French Embassy in Canada.

List of symbols

a	specific transfer surface area, 1/m
C	volumetric concentration, mol/m^3
d	diameter, m
D	diffusion coefficient, m^2/sec
H	Henry's law constant, Pa-m^3/mol
J	flux, mol/m^2-sec
K	mass transfer coefficient, m/sec
P	permeability, mol/m-sec-Pa
p	partial pressure, Pa
r	radius, m
R	gas law constant, 8.314 J/K mol
Re	Reynolds number, dimensionless
S	partition coefficient, dimensionless
S'	partition coefficient, mol/m^3 Pa
Sc	Schmidt number, dimensionless
Sh	Sherwood number, dimensionless
t	time, sec
T	temperature, K
v	velocity, m/sec

Greek letters

τ	membrane thickness, m
ν	kinematic viscosity, m^2/sec

Subscripts and superscripts

e	equivalent
E	equilibrium
G	gas
M	membrane
L	liquid
–	average

References

1 P.L. Côté, J.-L. Bersillon, A. Huyard and J.-M. Faup, Bubble-free aeration using membranes: Process analysis, J. Water Pollut. Control Fed., 60 (1988) 1986-1992.
2 R.B. Schaffer, F.V. Ludzack and M.B. Ettinger, Sewage treatment by oxygenation through permeable plastic films, J. Water Pollut. Control Fed., 32 (1960) 939-941.
3 W.L. Robb, Thin silicone membranes — their permeation properties and some applications, Ann. N.Y. Acad. Sci., (1965) 119-135.
4 H. Yasuda and C.E. Lamaze, Transfer of gas to dissolved oxygen in water via porous and nonporous polymer membranes, J. Appl. Polym. Sci., 16 (1972) 595-601.
5 T.E.-S. Tang, Mass transfer of dissolved bases through membrane tubing, Ph.D. Thesis, University of Iowa, Iowa City, 1975.
6 J. Lehmann, G.W. Piehl, R. Schulz and R.S. Braunschweig, Bubble free cell culture aeration with porous moving membranes, Special publication, Biotech-Forum, 2(3) (1985).
7 P.A. Wilderer, J. Braeutigam and I. Sekoulov, Application of gas permeable membranes for auxiliary oxygenation of sequencing batch reactors, Conserv. Recycling, 8 (1985) 181-192.
8 J. Crank and G.S. Park (Eds.), Diffusion in Polymers, Academic Press, London and New York, 1968.
9 E.L. Cussler, Diffusion, Mass Transfer in Fluid Systems, Cambridge University Press, Cambridge, MA, 1984.
10 T. Yamane, M. Matsuda and E. Sada, Application of porous Teflon tubing method to automatic fed-batch culture of microorganisms. I. Mass transfer through porous Teflon tubing, Biotechnol. Bioeng., 23 (1981) 2493-2507.
11 M.N. Ozisik, Basic Heat Transfer, McGraw-Hill, New York, NY, 1977.
12 A.G. Boon, Measurement of aerator performance, Symposium on the Profitable Aeration of Wastewater, London, 1980.
13 M.K. Stenstrom and R.G. Gilbert, Effect of alpha, beta and theta factor upon the design, specification and operation of aeration systems, Water Res., 15 (1981) 643-654.
14 Ming-Chien Yang and E.L. Cussler, Designing hollow-fiber contactors, AIChE J., 32 (1986) 1910-1916.